Electronic Supplementary Material (ESI) for Sensors & Diagnostics.

Supporting Information

Ultra-Sensitive Detection of PFASs using Surface Enhanced Raman Scattering: A Promising Approach for Environmental Analysis

Joshua C. Rothstein,[a] Jiaheng Cui,[b] Yanjun Yang,[b] Xianyan Chen,[c] and Yiping Zhao[a]

[a] Department of Physics and Astronomy, Franklin College of Arts and Sciences

[b] School of Electrical and Computer Engineering, College of Engineering

[c] Department of Epidemiology & Biostatistics, College of Public Health

The University of Georgia, Athens, GA, USA 30602

S1. SEM image of an AgNR substrate

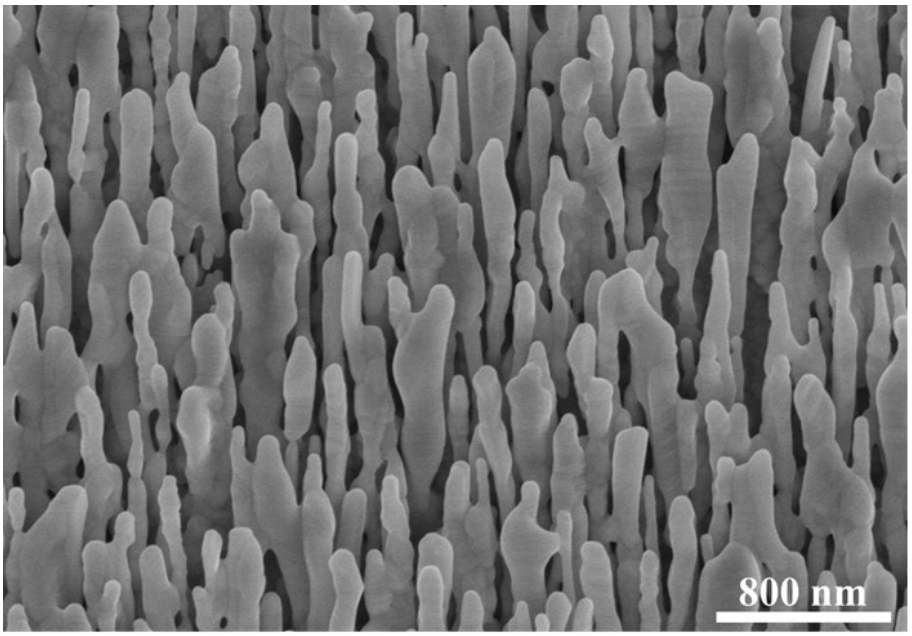

Fig. S1 A typical SEM image of the AgNR substrate.

S2. Optimization of MCH functionalization

To determine the optimal concentration of MCH, the MCH solution was diluted to the following 8 concentrations: 6, 15, 30, 60, 150, 240, 300, and 360 μM, respectively. 20 μL of each solution was pipetted to an AgNR well and incubated for an hour. Then, each well was rinsed with DI water and air-dried. 20 SERS spectra were taken from each well at each concentration with a laser power of 14.5 mW, a 20× objective lens, and 10 s acquisition time. The average spectra of these concentrations are shown in **Figure S2a**. The average peak intensities, along with their corresponding standard deviations at $\Delta\nu$ = 698, 869, and 1087 cm^{-1} were analyzed, as shown in **Figures S2b-d.**

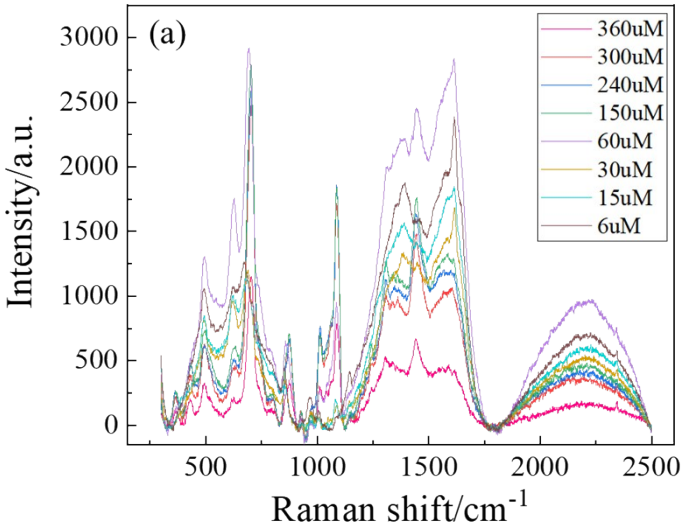

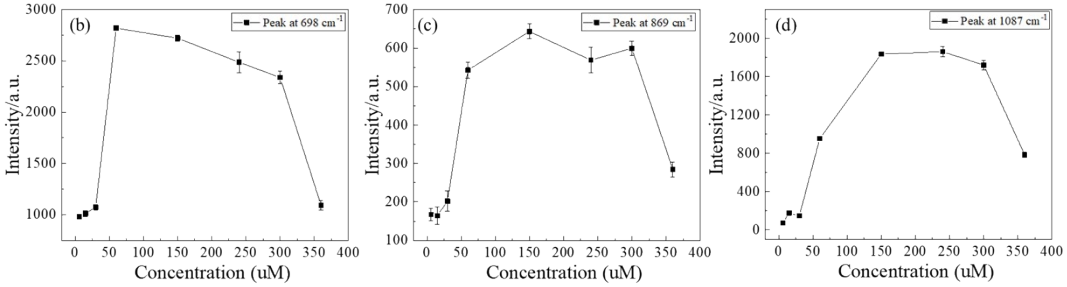

Fig. S2 (a) Baseline removed average spectra of MCH on AgNR at 8 concentrations. The following graphs track peak intensities of each concentration at (b) $\Delta\nu$ = 698 cm^{-1}, (c) $\Delta\nu$ = 869 cm^{-1}, and (d) $\Delta\nu$ = 1087 cm^{-1}.

S3. The comparison of the experimental and DFT Raman spectra of selected PFAS

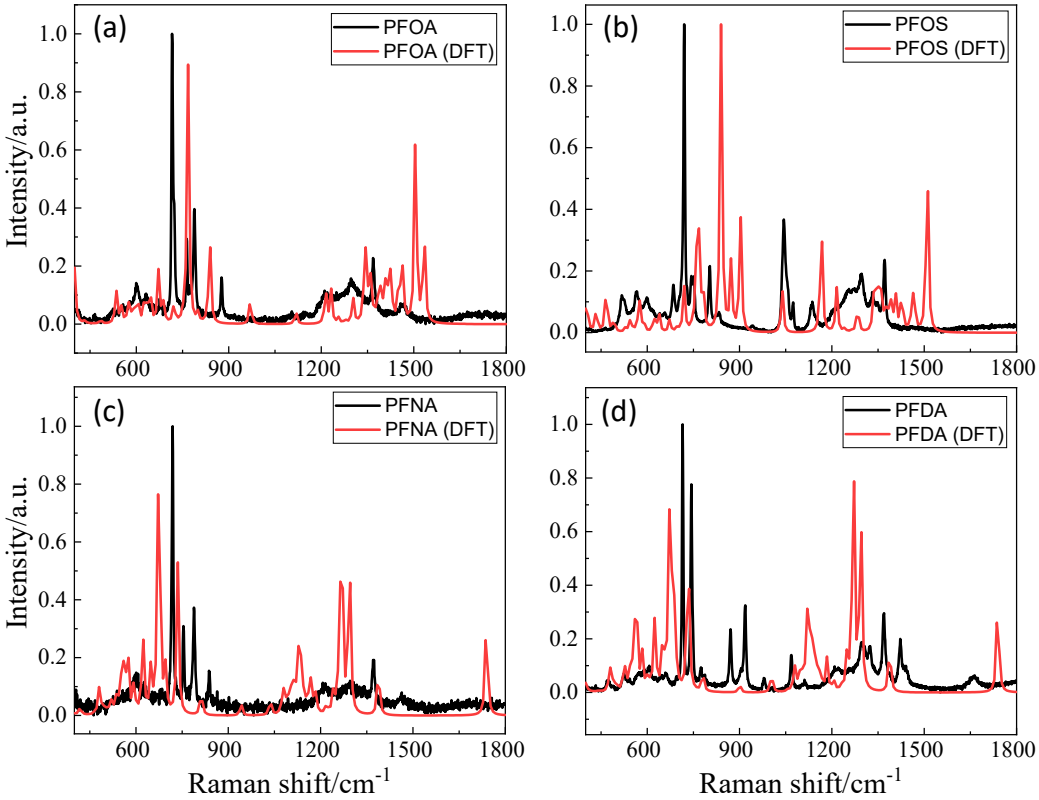

Fig. S3 Comparison of experimental obtained SERS spectra and those calculated using DFT. The DFT results are adapted from Chen et al.[1]

S4. List of peaks of PFAS SERS spectra

Table S1. A list of peaks of SERS spectra from five 10^3 ppt PFAS compounds in methanol as well as from an AgNR substrate, as shown in **Figure 3**.

HFPO-DA	PFDA	PFNA	PFOS	PFOA	AgNR
745	745	745	745	745	
805	805	805	805	805	805
927	927	927	927	927	927
999	999	999	999	999	999
1136	1136	1136	1136	1136	1136
1271	1271	1271	1271	1271	

1404	1404	1404	1404	1404	1404
1603	1603	1603	1603	1603	1603

S5. Cosine similarity matrix of PFAS SERS spectra

Table S2. Cosine similarity matrix between the spectra of the AgNR background and the PFAS samples (PFOA, PFOS, PFNA, PFDA, and HFPO-DA) shown in **Figure 3a**.

	AgNR	**PFOA**	**PFOS**	**PFNA**	**PFDA**	**HFPO-DA**
AgNR	1.000	0.643	0.618	0.618	0.659	0.619
PFOA	0.643	1.000	0.988	0.985	0.966	0.947
PFOS	0.618	0.988	1.000	0.993	0.982	0.967
PFNA	0.618	0.985	0.993	1.000	0.992	0.979
PFDA	0.659	0.966	0.982	0.992	1.000	0.990
HFPO-DA	0.619	0.947	0.967	0.979	0.990	1.000

S6. List of peaks of PFOA SERS spectra

Table S3. A list of peaks of SERS spectra for PFOA that appears throughout the paper. **Figure 2** presents the experimental Raman spectra of PFOA powder. **Figure 3a** shows the first experimental set of SERS spectra of PFOA with methanol, fixed at 10^3 ppt. **Figure 4a** displays the second experimental set of SERS spectra of PFOA with methanol, containing the concentrations 10^0, 10^1, 10^3, 10^6, 10^7, and 10^8 ppt. The highlighted cells represent the characteristic peaks shown in **Figure 4b**. The last column indicates the characteristic peaks of the reference, i.e., methanol, in **Figure 4b**.

PFOA			
Fig. 2	**Fig. 3a**	**Fig. 4a**	**Reference (methanol)**
		333	
			435
		485	
600		604	
630			
660			
675		682	682
715			
763	754	760	764
788			
	805		
		814	816
873		878	881
	927	934	934
	999	1005	1005
		1053	1053
	1136	1136	
	1271		
1296			
1370			
	1404	1403	1403
		1544	

	1603		
		1642	1642

S7. Cosine similarity matrix of PFOA SERS spectra

Table S4. Cosine similarity matrix between the reference spectrum and the spectra of different concentrations of PFOA shown in **Figure 4a**.

	Reference	**10^0 ppt**	**10^1 ppt**	**10^3 ppt**	**10^6 ppt**	**10^7 ppt**	**10^8 ppt**
Reference	1.000	0.778	0.717	0.775	0.713	0.734	0.774
10^0 ppt	0.778	1.000	0.970	0.996	0.961	0.977	0.969
10^1 ppt	0.717	0.970	1.000	0.978	0.998	0.998	0.932
10^3 ppt	0.775	0.996	0.978	1.000	0.970	0.983	0.961
10^6 ppt	0.713	0.961	0.998	0.970	1.000	0.996	0.919
10^7 ppt	0.734	0.977	0.998	0.983	0.996	1.000	0.947
10^8 ppt	0.774	0.969	0.932	0.961	0.919	0.947	1.000

S8. Peak locations and confusion matrix of PFAS on cysteine-modified AgNR substrates

Table S5. Center positions of the distinct peaks identified in the SERS spectra of PFOS and PFOA, and their presence in each spectrum shown in **Figure 5**.

Wavenumber (cm^{-1})	**PFOA**			**PFOS**			**Water**
-	10^8 ppt	10^4 ppt	10^{-2} ppt	10^8 ppt	10^4 ppt	10^{-2} ppt	-
502	√	√	√	√	√	√	√
672	√	√	√	√	√	√	√
724	√	√	√				
750	√	√	√	√	√	√	√
840	√						
857		√	√	√	√	√	√
904	√						
915				√			√
1050	√	√	√	√	√	√	√
1164	√	√	√	√	√	√	√
1230	√	√	√	√	√	√	√
1304	√	√	√	√	√	√	√
1354	√	√	√				
1399	√	√	√	√	√	√	√
1520				√	√	√	

1576	√	√	√				
1622	√	√	√	√	√	√	√

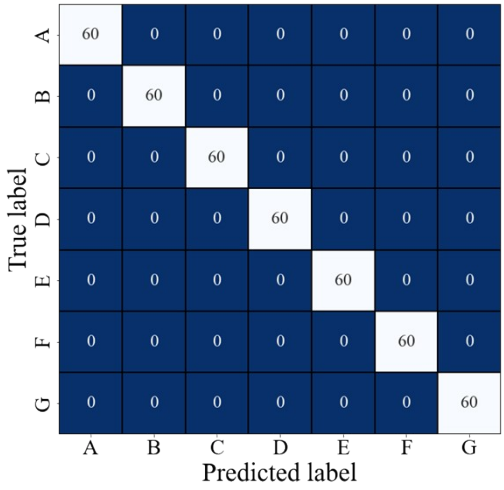

Fig. S4 The confusion matrix from an SVM model to process all spectra in **Figure 5**. Labels A, B, and C represent 10^8, 10^4, and 10^{-2} ppt PFOA; D, E, and F refer to 10^8, 10^4, and 10^{-2} ppt PFOS; and G is water on cysteine-modified AgNR substrates.

S9. Peak intensities of concentration-dependent baseline removed spectra

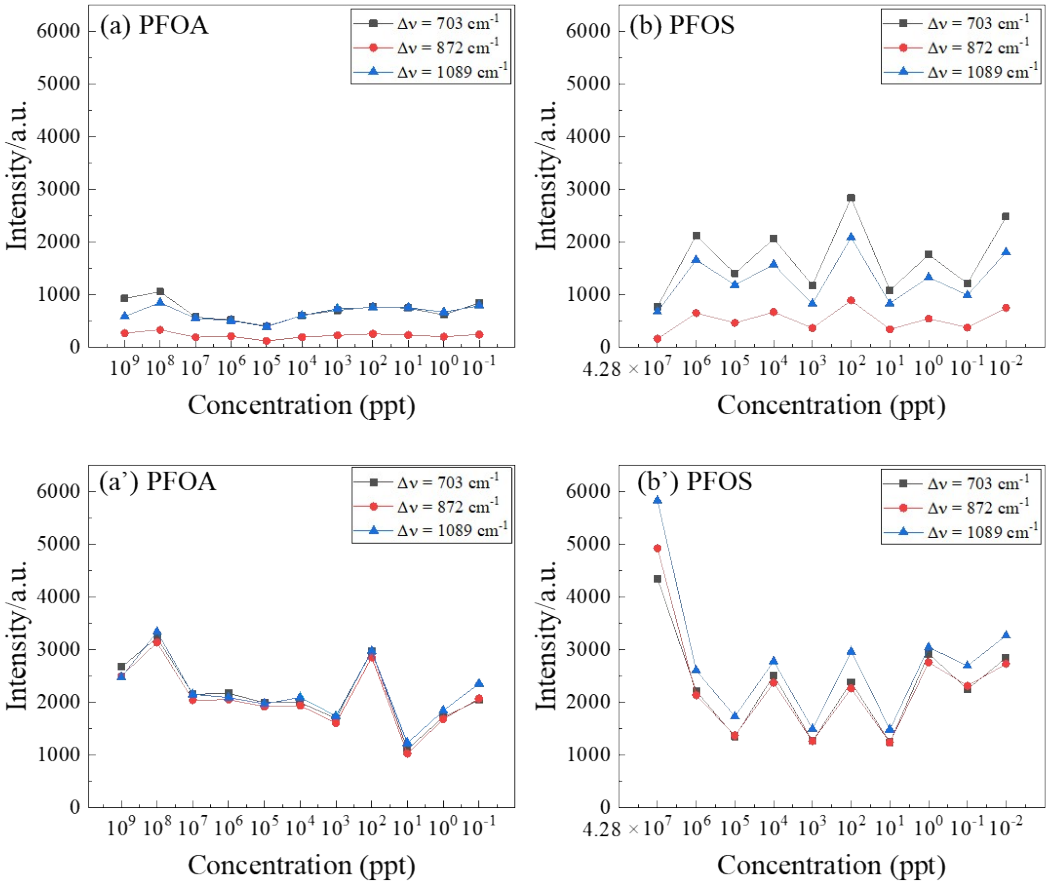

Fig. S5 The semi-log plot of the peak intensities at $\Delta\nu$ = 703, 872, and 1089 cm^{-1} versus concentration under these conditions: (a) PFOA with global baseline removal, (b) PFOS with global baseline removal; (a') PFOA with local baseline removal, (b') PFOS with local baseline removal.

References

1. Y. Chen, Y. Yang, J. Cui, H. Zhang and Y. Zhao, *Journal of Hazardous Materials*, 2024, **465**, 133260.